532.529:532.595

Paper No. 174-9

Oscillatory Flow Instabilities in Air-Water Two-Phase Flow System*

(1st Report Pressure Drop Oscillation)

By Mamoru OZAWA**, Koji AKAGAWA***, Tadashi SAKAGUCHI***, Toshiro TSUKAHARA† and Terushige FUJII††

The purpose of this study is to make clear the flow instability problem in two-phase flow systems. In this first report, an experimental study was conducted on the oscillatory flow instabilities in an air-water two-phase flow system with upstream compressible volume. The flow pattern during the oscillation and the effects of the compressible volume and the average superficial velocity on the limit cycles were investigated. The periods of the oscillations were well correlated by two characteristic parameters obtained from a simple non-linear analysis.

1. Introduction

There have been many analytical and experimental investigations on the flow instabilities in boiling two-phase flow systems. There are several types of instabilities such as density wave oscillation, flow pattern transition instability, pressure drop oscillation, thermal oscillation, geysering, etc. as described by Boure et al.[1] Some of the mechanisms of these oscillations have been studied and the threshold conditions of flow instabilities can be predicted reasonably,[2] but these are limited to the linear oscillation such as the density wave oscillation. On the contrary, there are few investigations on the flow oscillations caused by the non-linearity of a two-phase flow and the mechanisms of oscillations are not well understood.

In this series of reports, the two-phase flow dynamics including flow oscillation in capillary tubes where the two-phase flow pattern has the dominant effect on the pressure drop characteristics is presented.

The steady state characteristics of a two-phase flow in a capillary tube have been already investigated by Suo et al.;[3] Akagawa et al.[4] and Ohya.[5] Akagawa et al.[6] and Ohya[7] reported that the flow oscillation was observed in a system with an upstream compressible volume, but the mechanisms and the characteristics of the oscillation were not fully investigated because of the limited range of the experiments.

This first report presents the experimental results on the flow oscillation occurring in a system constructed of a capillary tube in which an air-water mixture flows and where is sufficiently large compressible volume upstream of the capillary tube (V/V_p= 23.6-529). The relations between the limit cycle of the oscillation and the pressure drop vs. flow rate characteristics, the flow pattern transition and the period of the oscillation were discussed. Secondly, the mechanism of this oscillation was compared with that of the pressure drop oscillation which was observed in a boiling channel system.[8,9] Lastly, the correlation of the oscillation period based on a lumped parameter non-linear analysis was presented.

* Received 15th March, 1978

** Researcher, Faculty of Engg., Kobe University, Kobe.
*** Professor, Faculty of Engg., Kobe University.
† Engineer, Hokushin Electric Works, Ltd.
†† Researcher, Faculty of Engg., Kobe University.

Nomenclature

V : compressible Volume
V_p : volume in the test section
D : inner diameter of the test tube
w_{go} : superficial velocity of air
w_{lo} : superficial velocity of water
ΔP : pressure drop in the test section
P_o : pressure at the inlet of the compressible volume
P' : pressure in the compressible volume
P : pressure at the exit of the test section
w_{gs} : air velocity in the air supply line to the compressible volume
L : test tube length
L' : length of the air supply line to the compressible volume
A : cross sectional area of the test tube
A' : cross sectional area of the air supply line
γ_g : specific weight of air
γ_l : specific weight of water
g : gravitational acceleration
w_{go}^{a} : superficial air velocity when the pressure drop has a maximum value
w_{go}^{b} : superficial air velocity when the pressure drop has a minimum value
α : constant value

Superscript
$-$: time averaged value

2. Experimental apparatus

The experimental apparatus is shown in Fig.1. The principal parts of the apparatus are an overflow tank [1], a compressor [4], a mixing section [3], a compressible volume [8] and a test section [9]. Water from the overflow tank is fed into the mixing section through the needle valve V_1 where the flow rate of water is adjusted to the predetermined value. Air flow from the compressor is regulated by the pressure regulator [5] and the critical flow nozzle [6] and is fed into the mixing section [3] through the injection needle of 1.0 mm I.D. A two-phase misture formed in the mixing section flows through the horizontal test section and is ejected into the atmosphere. Experiments were carried out on two test sections of capillary galss tubes of dimensions of 3.18 mm I.D. and 3.10 m length between two pressure taps [10] and 1.99 mm I.D. and 3.08 m length. The inner surface of the test section of is smooth and the friction factor measured in each test tube agreed well with the value by the equation 64/(Reynolds number) in the laminer flow region. The void fluctuation is detected by the capacitance void probes [11] at four locations along the test tube. The compressible volume is connected to the system between the critical flow nozzle and the hot wire probe. By closing the valve V_3, the compressible volume can be isolated from the system. The water flow rate and the air flow rate were measured by the hot film probe [2] and the hot wire probe [7] respectively and were also measured directly at the exit of the test section by measuring the volume flow rates. As the pressure drop at the valve V_1 was very large compared with the pressure drop in the test section, the water flow rate at the inlet was maintained constant regardless of the pressure fluctuation in the test section. The air flow rate was kept constant by the critical flow nozzle.

The differential pressure at the test section was measured by the D.P, cell [12] and was recorded by the oscillograph simultaneously with the air flow rate, the water flow rate and the four void signals.

3. Experimental procedure

An experiment was conducted according to the following procedure.

Firstly, the hot film probe and the hot wire probe were carefully calibrated. The friction loss was measured under the condition of single phase flow of water and it was confirmed that there was no change in the inner surface condition of the test tube.

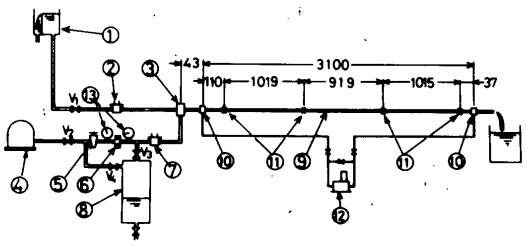

Fig.1 Experimental apparatus

Secondly, static characteristics of the frictional pressure drop was obtained by adjusting the water flow rate to a predetermined value and changing the air flow rate with a small increment. Thirdly, for the instability tests the air flow rate was brought to a predetermined state in the negative slope region of the pressure drop vs. flow rate relation, and the compressible volume was connected to the system by opening the valve V_3. The variations in the pressure drop, air velocity and water velocity were measured simultaneously after the oscillation settled to steady state. The volume in the compressible volume was changed by filling the tank with water.

After one series of experiments, the pressure drop under the water single phase flow was measured and the hot wire and the hot film probes were calibrated to confirm the calibration curves.

Four series of experiments were carried out with a test tube of D =3.18 mm and three series with a test tube of D =1.99 mm

Experimental condition was: superficial water velocity w_{lo}=0.0945～0.403 m/s and superficial air velocity w_{go} =0～1.1 m/s for the tube of D =3.18 mm and w_{lo}=0.0965 ~ 0.289 m/s, w_{go} =0 ~ 1.2 m/s for the tube of D = 1.99 mm The water and the air temperatures were from 13 °C to 15 °C.

4. Static characteristics of the pressure drop and flow pattern

As the static characteristics of the pressure drop of the two phase flow in a capillary tube were reported in the previous paper[4], the relation between the pressure

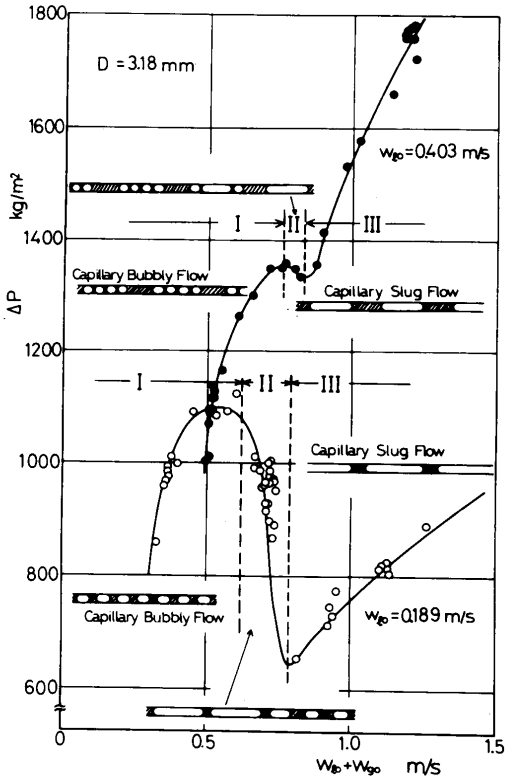

Fig.2 Static characteristics of pressuredrop

drop and the flow pattern is mainly discussed in this paper.

In Fig.2, the pressure drops in a two-phase flow are plotted against the superficial velocity of the two-phase flow $w_{go} + w_{lo}$. In every case of w_{lo} =1.89, 0.277 and 0.403 m/s the pressure drop vs. superficial velocity curves are divided into three regions: regions where ΔP increases with an increasing superficial velocity, (I) and (III); and a region where ΔP decreases with an increasing superficial velocity, (II). In the region (I) the small bubbles, which almost occupy the tube cross section, flow with an approximately constant pitch and travel at a uniform velocity. (This flow pattern is referred to as the capillary bubbly flow). In the region (III) the bubble is very long compared with the tube diameter. (This flow pattern is referred to as the capillary slug flow). The bubble becomes longer with an increase in w_{go} and the capillary slug flow transforms into an annular flow.

The region (II) is the transition state from region (I) to (III), and in this region the capillary bubbles coalesce travelling the tube and capillary slugs are formed. The steady state data points were obtained in the previous experiments[4] in which an air injection nozzle of very small diameter at the mixing section was used and the nozzle acted as a critical flow nozzle and the air flow rate did not change regardless of the pressure drop in the test section. But in this experiment a flow oscillation with a small amplitude occurred in the region (II) as shown in Fig.4, because the inner volume of the tube from the critical nozzle to the mixing section, which was about 14 cm^3, acted as the compressible volume. The flow pattern changed periodically from the capillary bubbly flow to the capillary slug flow during the flow oscillation. Therefore, the experimental data on the region (II) in this report are time averaged values. The bubbles in the region (III) flow with equal pitch at every w_{lo}. And the bubbles in the region (I) flow with equal pitch at w_{lo} = 0.189 and 0.277 m/s, and those at w_{lo} = o.403 m/s flow intermittently.

The relationships between the pressure drop and the flow pattern were also investigated by Inoue et al.[10] with far larger diameter tubes of 5.0 ~ 28.8 mm and by Ohya[5] with capillary tubes of 2.0 ~ 6.0 mm.

The region (I) in this paper corresponds to the bubbly flow region defined by Inoue et al.[10] and to the total range of the bubbly flow, simple slug and the imbricate slug regions defined by Ohya;[5] the region (III) corresponds to the slug flow and the annular flow regions defined by Inoue et al.[10] and to the annular flow region by Ohya;[5] and lastly the region (II) corresponds to the froth flow region by Ohya.[5]

5. General feature of flow oscillation

In Fig.3, typical oscillation traces of the air flow rate at the inlet and the differential pressure in the test section are shown. These oscillations were obtained under the time averaged superficial velocity of air $\bar{w}_{go}$ = 0.534 m/s, V = 3070, 4070 and 5070 cm^3, and the hypothetical equilibrium state was at about the middle point of the region (II).

The oscillation periods are relatively long, being about 200 ~ 300 sec. The period increases with an increase in the compressible volume. The cycle of the air flow rate consists of 4 processes: (A) rapid increase to the maximum, (B) gradual decrease accompanied by a high-frequency oscillation,

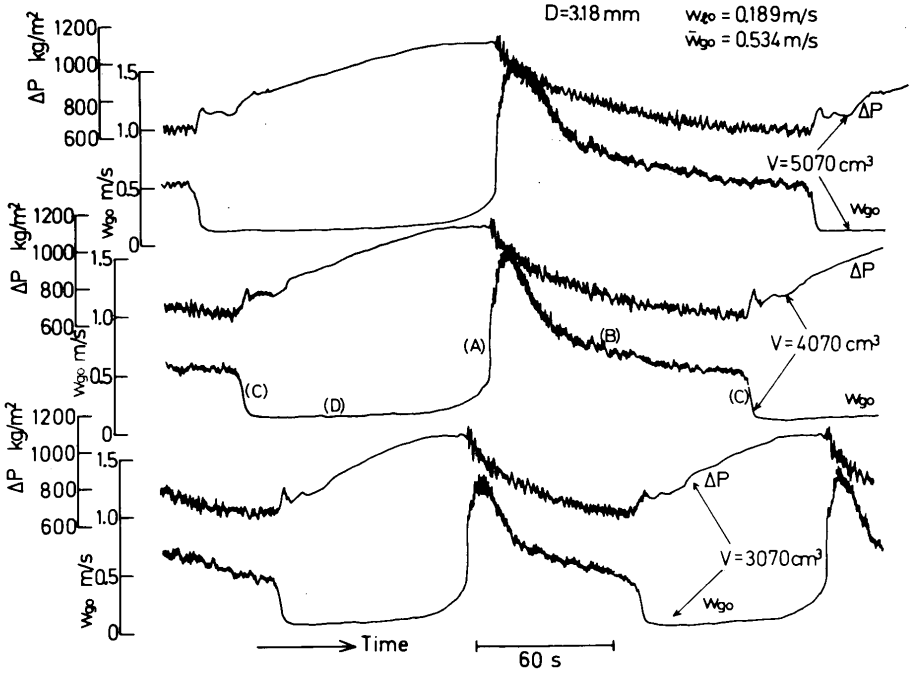

Fig.3 Oscillation recordings

(C) rapid decrease and (D) gradual increase from the minimum value. The differential pressure changes corresponding to the variation of the air flow rate and increases in the processes (C) (D) and (A), and decreases in the process (B) as can be seen in Fig.3. The high-frequency oscillations of ΔP and w_{go} in the process (B) and a part of (A) are caused by the capillary slug flow.

In Fig.4, typical oscillation traces in the case of the compressible volume of V = 14 cm^3 are shown. This oscillation was also obtained under the time averaged superficial velocity of air $\bar{w}_{go}$ = 0.534 m/s and the hypothetical equilibrium state was in the region (II). The oscillation period is very small compared with those in Fig.3. As can be seen in Fig.4 though the water superficial velocity does not change and is constant at 0.189 m/s, the air superficial velocity and the differential pressure fluctuate and the variations of w_{go} and ΔP are out of phase.

In this case the four processes described above are not observed in the cycle of the superfical air velocity. The void signals were obtained at the locations of Z = 110 mm, 1129, 2048 and 3063 from the pressure tap of the upstream side. In the void signals, the high requency oscillations with small amplitude correspond to the capillary bubble and the large fluctuations correspond to the capillary slug. When the superficial velocity w_{go} begins to increase, at first the flow pattern transition from the capillary bubbly flow to the capillary slug flow occurs at the inlet and the exit of the tube simultaneously and these transition points spread in two directions: from the upstream to the downstream and from the downstream to the upstream. The transition from the capillary bubbly flow to the capillary slug flow at the exit side is due to the agglomeration of the bubbles. The transition of the flow pattern from the upstream to the downstream is due to an increase of the air flow rate against the constant water flow rate. When the superficial velocity begins to decrease, the flow pattern from capillary slug flow to capillary bubbly flow spreads in the inlet downstream direction.

From this experiment, it is concluded that the flow oscillation occurs in the existence of even a very small compressible volume when the hypothetical equilibrium state is in the negative slope region of the pressure drop vs. supperficial velocity curve. Accordingly there is a possibility that the flow oscillation occurs in a channel system accompanied by a mixing of gas and liquid.

6. Limit cycle and flow pattern

The limit cycle of the oscillation, which was obtained by plotting the values of pressure drop against the two-phase superficial velocity ($w_{go} + w_{lo}$) during the oscillation is shown in Fig.5. The transi-

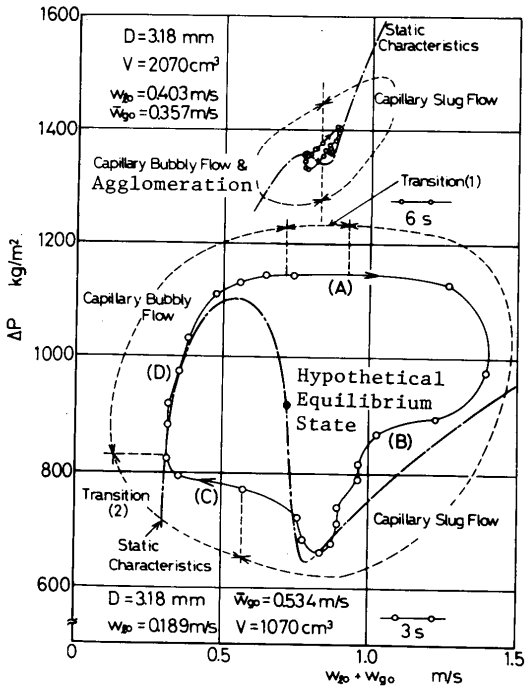

Fig.5 Limit cycle and flow pattern

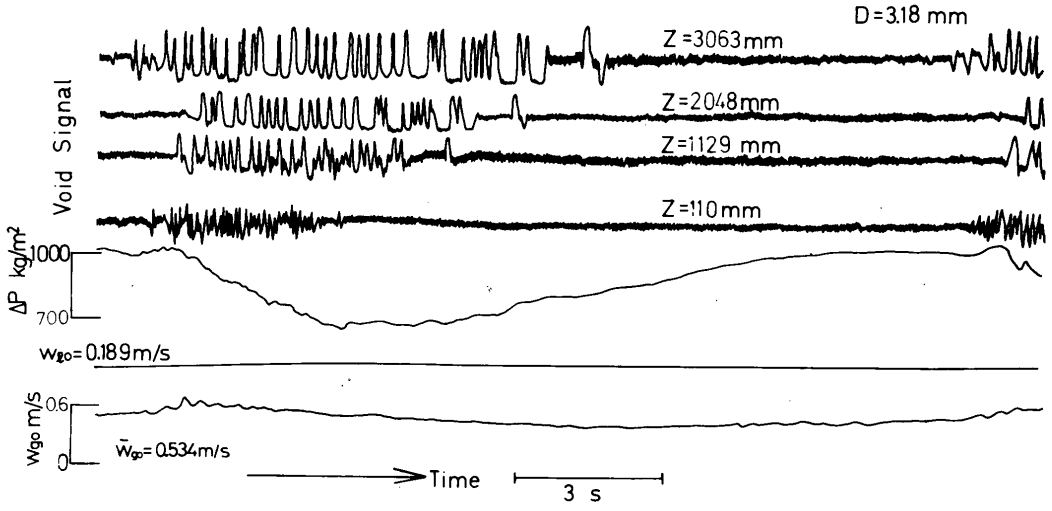

Fig.4 Oscillation recordings

ent state on the limit cycle moves along approximately a static characteristic curve in the positive slope region (the region (I) and (III) in Fig.2) as shown in (B) and (D), and the flow excursions occur in the negative slope region (the region (II)) as shown in (A) and (C). The states designates by the symbols A, B, C and D in Fig.5 correspond to the states designated by A, B, C and D in Fig.3. In the case of w_{lo} = 0.189 m/s, the flow pattern changes along the limit cycle in the order of the capillary bubbly flow, the transition (1), the capillary slug flow, the transition (2) and the capillary bubbly flow. In the region of the transition (1), the flow pattern transition spreads in two directions: the transition owing to the agglomeration of small bubbles spreads from the exit side to the inlet side, and the transition with the flow spreads from the inlet side to the exit side. In the transition (2), the flow pattern transition spreads from the inlet side to the exit side with the flow.

In the case of w_{lo} = 0.403, the negative slope region (II) is very small compared with that in the case of w_{lo} = 0.189 m/s. Therefore the limit cycle on the ΔP vs. $w_{go}+w_{lo}$ plane is also small. According to the flow pattern the limit cycle divided into two regions: the region of the capillary slug flow and the region where the capillary bubbly flow exit in the upstream and the agglometration occurs in the downstream.

The limit cycle in the case without a compressible volume [8] but with a small compressible volume of the air supply line of V = 14 cm^3 is shown in Fig.6. The transient state moves on the limit cycle in the direction designated by the arrow and the flow pattern changes in the order of the capillary bubbly flow, the transition (1), the capillary slug flow, the transition (2) and the capillary bubbly flow. In the transition (1) the flow pattern transition owing to the agglomeration of bubbles and that with a flow simultaneously occur, and in the transition (2) the flow pattern changes with the flow. These tendencies of the flow pattern transition were also observed in another experimental run of a different inner diameter or superficial water velocity.

The oscillation trace and the limit cycle shown in Figs.3 and 5 respectively are very similar to those of the pressure drop oscillation observed in the boiling channel system with R-113[9]. The tendency that the oscillation period increases with the compressible volume agrees with that of the pressure drop oscillation. The oscillations in both cases occur in the negarive slope region on the ΔP vs. $w_{go}+w_{lo}$ curve. Therefore, the oscillatory flow instability in this experiment is defined as the pressure drop oscillation caused by the dynamic interactions between the nonlinear characteristics of pressure drop with negative slope region in two-phase flow and the upstream compressible volume.

7. Effects of various parameters on limit cycle

7.1 Compressible volume

The limit cycles of the pressure drop oscillation for various values of compressible volume V are drawn on the ΔP vs. $w_{go}+w_{lo}$ plane in Figs.7 and 8. When the compressible volume is as small as 14 cm^3, the limit cycles stay in the region (II) of

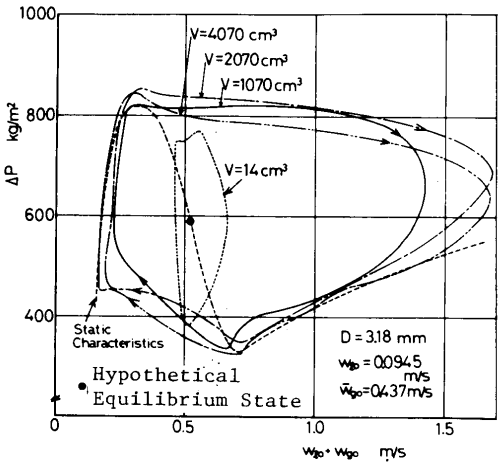

Fig.7 Effect of compressible volume

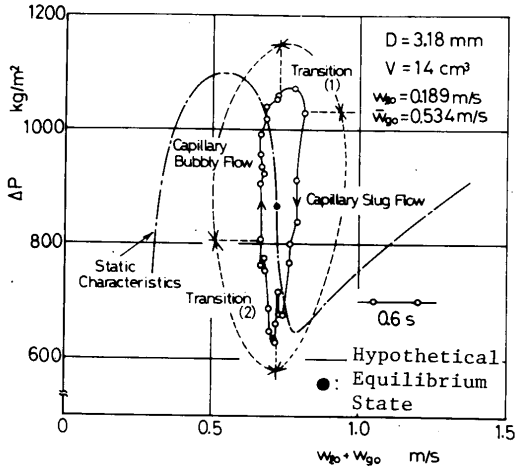

Fig.6 Limit cycle and flow pattern

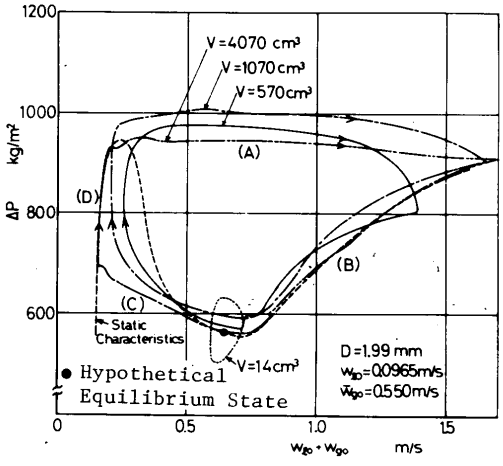

Fig.8 Effect of compressible volume

the pressure drop vs. superficial velocity curve. The limit cycle becomes larger with an increase in the compressible volume and the limit cycle comes almost to coincide with the static characteristic curve in the regions (I) and (III) in the case of V = 4010 cm^3.

The superficial velocities at time t and $t+\delta t$ are designated by $w_{go}|_t$ and $w_{go}|_{t+\delta t}$ respectively and the average acceleration during the time from t to $t+\delta t$ is given by $(w_{go}|_{t+\delta t} - w_{go}|_t)/\delta t$ When the time period of sampling δt is sufficiently small compared with the oscillation period, then $(w_{go}|_{t+\delta t} - w_{go}|_t)/\delta t$ becomes approximately equal to the time derivative of w_{go} (in this experiment, w_{go} was maintained constant. Therefore, the time derivation of w_{go} is equal to that of $w_{go} + w_{lo}$). In Fig.9, the time derivative $d(w_{go}+w_{lo})/dt$ obtained from the oscillation recordings is plotted against $w_{lo}/(w_{go}+w_{lo})$ during 1 cycle of the oscillation. The value $w_{lo}/(w_{go}+w_{lo})$ is nearly equal to the hold up (1-void fraction) because the slip ratio is approximately equal to unity in this capillary tube, and the value $w_{lo}/(w_{go}+w_{lo})\cdot V\cdot$(density of water) represents approximately the mass in the test section. Each curve in Fig.9 corresponds to that in Fig.8 and the state represented by A ~ D corresponds to that in Fig.8. The state changes in the order of A, B, C and D. In the states A and C, the flow excursions occur. The absolute value of the acceleration at the state (A) is larger than that at (C). This shows that the excursion at A is faster than that at C. The speed of the excursion depends also on the hypothetical equilibrium state as is described in the following section.

The absolute value of the acceleration at B is relatively larger than that at D. This is mainly due to the fact that the mass at B is smaller than that at D. And the absolute values of acceleration at B and D decrease with an increase in the compressible volume, showing that the state moves more slowly in the regions (I) and (III), in other words, the state in the regions (I) and (III) approaches a quasi-steady state with an increase in the compressible volume.

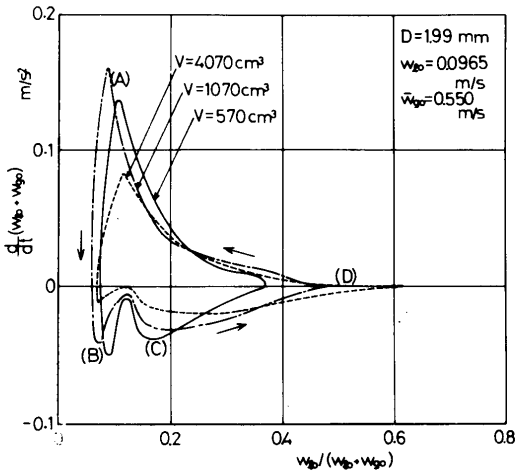

Fig.9 Acceleration during the oscillation

7.2 Effect of hypotherical equilibrim state point

The experimental results in the case of D = 1.99 mm are shown on the phase plane, i.e. $d(w_{go}+w_{lo})/dt$ vs. $w_{go} + w_{lo}$, in Fig.10. In the case of the time ageraged superficial velocity $\bar{w}_{go}$ = 0.502 m/s, the hypothetical equilibrium state which is designated by the solid circle ( ) is located in the middle of the negative slope of the ΔP vs. $w_{go} + w_{lo}$ plane, and the locus on the phase plane is approximately symmetric with respect to the equilibrium state point designated by solid point. This shows that the speeds of excursion in the processes (A) and (C) are approximately equal to each other. On the contrary, in the case of $\bar{w}_{go}$ = 0.585, the hypothetical equilibrium state point is located in the right side of the negative slope, then the locus on the phase plane is unsymmetric with respect to the equilibrium state point designated by the circle. This shows that the speed of excursion in the process A is faster than that in the process C. When the equilibrium state is in the left side of the negative slope, the speed of excursion in the process C may become faster than that in the process A.

A simple analysis by a lumped parameter model is shown in order to explain the effect of the location of the hypothetical equilibrium state point on the oscillation qualitatively. As the resistance at the inlet of the compressible volume is very small in this experimental apparatus, this resistance is neglected for simplicity. The mass in the test tube is assumed to be constant during the oscillation under the assumption of the lumped parameter model. Then the momentum equation is written as follows:

$$P_0 - P' = I' \frac{dw_{go}'}{dt} \quad \cdots\cdots(1)$$

$$P_0 - P = I \frac{dw_{go}}{dt} + \Delta P \quad \cdots\cdots(2)$$

where

$w_{go}' = w_{gs} A'/A$

$I' = L'A\gamma_g / gA'$

$I = L(w_{lo}\gamma_l + w_{go}\gamma_g)/\{g(w_{lo} + w_{go})\}$

As the state of air in the compressible volume changes isothermally,

$$w_{go}' = c(dP'/dt) \quad \cdots\cdots(3)$$

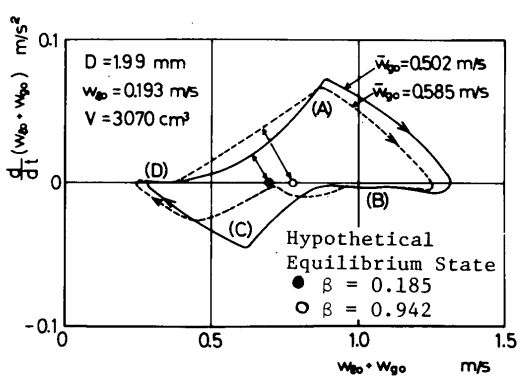

Fig.10 Effect of hypothetical equilibrium state

where $c = V/(AP')$ and c is assumed to be constant during the oscillation. Then the static characteristics of the pressure drop can be approximated by the following equation,

$$d(\Delta P)/dw_{g0}=\alpha(w_{g0}-w_{g0}^{a})(w_{g0}-w_{g0}^{b}) \quad \cdots(4)$$

From these equations (1), (2), (3) and (4), the dimensionless momentum equation is expressed by

$$\frac{d^2y^*}{dt^{*2}}-\varepsilon(1-2\beta y^*-y^{*2})\frac{dy^*}{dt^*}+y^*=0 \quad \cdots(5)$$

where

$$y^*=(w_{g0}-\bar{w}_{g0})/\sqrt{(\bar{w}_{g0}-w_{g0}^{a})(w_{g0}^{b}-\bar{w}_{g0})}$$

$$t^*=t/\tau, \qquad \tau=\sqrt{c(I+I')}$$

$$\varepsilon=-\sqrt{c/(I+I')}\,d(\Delta P)/dw_{g0}|_{\bar{w}_{g0}}$$

$$\beta=0.5(2\bar{w}_{g0}-w_{g0}^{a}-w_{g0}^{b})/\sqrt{(\bar{w}_{g0}-w_{g0}^{a})(w_{g0}^{b}-\bar{w}_{g0})}$$

The equation (5) has the same form as the equation which was derived for the pressure drop oscillation in the boiling channel system[9] by one of the authors. The characteristics of the limit cycle on the phase plane can be easily characterized by the dimensionless parameters ε and β. In the case of $\beta = 0$, Eq.(5) is reduced to a van der Pol equation, and the limit cycle is symmetric with respect to the origin on the phase plane dy^*/dt vs.y^*. In the case of $\beta \neq 0$, the limit cycle is unsymmetric with respect to the origin. The values of β are 0.185 and 0.942 under the conditions $\bar{w}_{g0}$ = 0.502 m/s and 0.585 m/s in Fig.11 respectively. From the characteristics of Eq.(5), it is shown that the limit cycle for β = 0.942 has more unsymmetric character than that for β = 0.185 and that the positive portion of $d(w_{g0} + w_{l0})/dt$ of the limet cycle is larger than the negative portion in the case of β = 0.942. These tendencies agree with the experimental results shown in Fig.11.

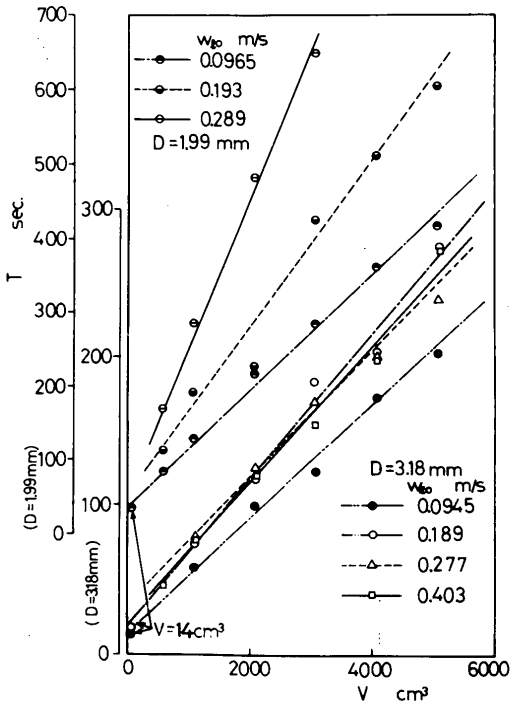

Fig.11 Oscillation period

When the value of β is positive the state of $w_{g0} > w_{l0}$ (almost coincides with the process B) occupies a larger portion of one cycle with an increase in the value of β on the trace of the oscillation of w_{g0}. On the contrary, when β is negative the portion with negative value of $d(w_{g0} + w_{l0})/dt$ on the limit cycle becomes larger than that with positive value. Thus the speed of excursion in the process C is faster than that in the process A and the state of $w_{g0} < \bar{w}_{g0}$ (almost coincides with the process D) occupies a relatively larger portion of one cycle of the oscillation. These tendencies also agree with those in the experiment.

8. Oscillation period

The oscillation periods T are plotted against the compressible volume V for the parameter w_{l0} in Fig.11. In the case of D = 3.18 mm, the period increases with an increase in the compressible volume but the effect of w_{l0} on the period is not seen in the range of 0.189 to 0.403 m/s. In Fig.11, the periods in the cases of w_{l0} = 0.189, 0.0945 (D = 3.18 mm) and 0.0965 m/s (D = 1.99 mm) and with a compressible volume of 14 cm^3 are also plotted. These data lie on the same lines for V = 570 ~ 5070 cm^3 respectively.

It is expected from Eq.(5) that the oscillation periods depend on the dimensionless parameter ε, then the experimental results on the oscillation period can be correlated by the parameter ε. The experimental values of T are normalized by the characteristic time constant $\tau = \sqrt{c\ (I+I')}$ then the dimensionless time T/τ is plotted against the parameter ε in Fig.12. The value of $d(\Delta P)/dw_{g0}|_{\bar{w}_{g0}}$ can be obtained by approximating the static characteristics of the pressure drop by Eq.(4) and by substituting the time ageraged superficial velocity $\bar{w}_{g0}$ into Eq.(4). But it is rather difficult to approximate the static characteristics of the pressure drop by the third order equation of w_{g0} as in the case of Fig.8. Therefore, in this paper the value of $d(\Delta P)/dw_{g0}|_{\bar{w}_{g0}}$ is chosen as an operating parameter for the simple correlation.

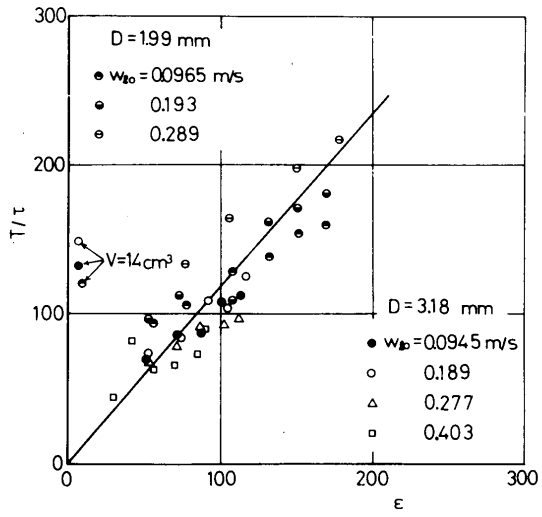

Fig.12 Dimensionless correlation of period

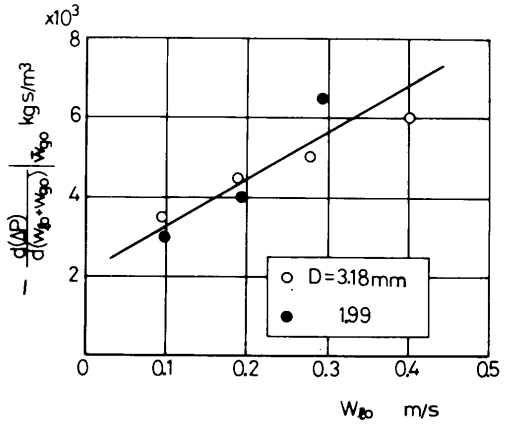

Fig.13 Operation parameter in the correlation

It can be seen that the data for V = 570 ~ 5070 cm^3 are well correlated by the parameter ε in Fig.12, but the data for V = 14 cm^3 cannot be correlated by this method. From these facts, when a system has a relatively large compressible volume, the oscillation can be well expressed by the lumped parameter model. The operating parameter $d(\Delta P)/dw_{g^o}|w_{g^o}$ used in Fig.12 is plotted aginst w_{l^o} in Fig. 13. It is seen that the operating parameter used here depends mainly on w_{l^o}. These values are the same order as the values of inclination of ΔP vs. $w_{g^o}+w_{l^o}$ curves obtained in the experiment.

9. Conclusions

An experimental study on the pressure drop oscillation in capillary tubes which was one of the typical nonlinear oscillations in a gas-liquid two-phase flow system was carried out with the conclusions summarized as follows:

(1) A pressure drop oscillation occurs when the hypothetical equilibrium state is in the negative slope region of the static characteristic curve of the pressure drop vs. superficial velocity. The flow pattern changes during the oscillation in the order of the capillary bubbly flow, the transition, the capillary slug flow, the transition and the capillary bubbly flow.

(2) The oscillation period increases with an increasing compressible volume.

(3) The locus of the limit cycle on the phase plane and the profile of the oscillation depend on the hypothetical equilibrium state.

(4) The pressure drop oscillation in this experiment can be expressed approximately by a similar equation to that in the boiling channel system.

(5) The dimensionless period T/τ is well correlated by the dimensionless parameter ε.

Authors wish to thank Mr. Hiroshi Oita for his assistance in carrying out the experiment. A part of this experiment was supported by the Fund of Scientific Research granted by the Japanese Ministry of Education.

References

(1) Bouré, J. A., et al., ASME Paper 71-HT-42 (1971), 1.
(2) Davies, A. L., Potter, R., EURATOM Report, Proc. Symp. on Two-Phase Flow Dynamics, Eindhoven (1967), 1225.
(3) Suo, M., Griffith, P., Trans. ASME, Ser. D, 86-3 (1964-9), 576.
(4) Akagawa, K., et al., Preprint of JSME (in Japanese), (38th in Kansai Branch), Part 2 (1963-3), 147.
(5) Ohya, T., Trans. JSME, 38-308 (1972-4), 767.
(6) Akagawa, K., et al., Preprint of JSME, No.109 (1964-3), 65.
(7) Ohya, T., Trans. JSME, 38-308 (1972-4), 790.
(8) Maulbetsch, J. S., Griffith, P., 3rd International Heat Transfer Conference, Chicago (1966), 247.
(9) Nakanishi, S., et al., Trans. JSME, 44-388 (1978-12), 4245.
(10) Inoue, A., Aoki, S., Trans. JSME, 32-238 (1966-6), 940.